

Multimodal Learning with Channel-Mixing and Masked Autoencoder on Facial Action Unit Detection

Xiang Zhang¹, Huiyuan Yang², Taoyue Wang¹, Xiaotian Li¹ and Lijun Yin¹

¹ State University of New York at Binghamton, NY, USA

² Rice University, TX, USA

Abstract—Recent studies utilizing multi-modal data aimed at building a robust model for facial Action Unit (AU) detection. However, due to the heterogeneity of multi-modal data, multi-modal representation learning becomes one of the main challenges. On one hand, it is difficult to extract the relevant features from multi-modalities by only one feature extractor, on the other hand, previous studies have not fully explored the potential of multi-modal fusion strategies. For example, early fusion usually required all modalities to be present during inference, while late fusion and middle fusion increased the network size for feature learning. In contrast to a large amount of work on late fusion, there are few works on early fusion to explore the channel information. This paper presents a novel multi-modal network called Multi-modal Channel-Mixing (MCM), as a pre-trained model to learn a robust representation in order to facilitate the multi-modal fusion. We evaluate the learned representation on a downstream task of automatic facial action units detection. Specifically, it is a single stream encoder network that uses a channel-mixing module in early fusion, requiring only one modality in the downstream detection task. We also utilize the masked ViT encoder to learn features from the fusion image and reconstruct back two modalities with two ViT decoders. We have conducted extensive experiments on two public datasets, known as BP4D and DISFA, to evaluate the effectiveness and robustness of the proposed multimodal framework. The results show our approach is comparable or superior to the state-of-the-art baseline methods.

I. INTRODUCTION

Facial Action Coding System (FACS) [9] is designed to detect subtle facial changes by describing facial muscle movement, while the combination of basic AUs (Action Units) characterizes human expressions. Automatic AUs detection has been studied for decades in human emotion analysis and human facial behavior analysis. AUs may occur individually or in combinations, hence AUs detection has been mainly treated as a multi-label classification problem, which is a challenge in computer vision.

By using 2D images, several methods achieve state-of-the-art performance in AU detection[19], [33], [29], [6], [16], [42], [15]. However, these supervised approaches are very scarce for labeled data, and AU annotation is a highly labor-intensive and time-consuming process, thus researchers attempt to utilize unlabeled data through self-supervised learning[27], [23]. Moreover, as some subtle facial muscle movements are not easily observed in the images, multimodal approaches are necessary for efficient AU detection. For instance, *AU6* (cheek raiser) involves the deformation of *Orbicularis oculi* and *pars orbitalis* muscles, which shows subtle differences when observed in images, but appears

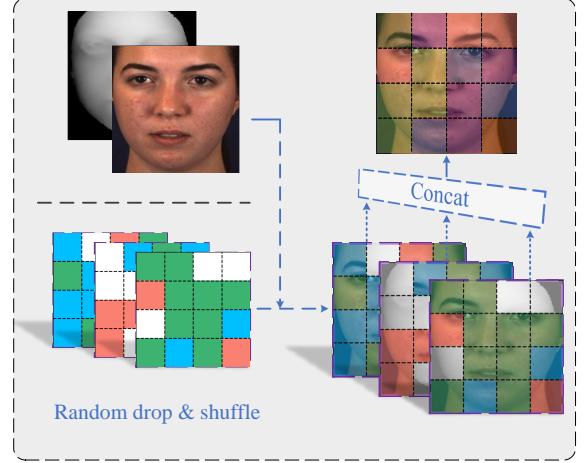


Fig. 1: Overview of Channel-Mixing module. First, visual and depth are concatenated by channel; Second, mix the channels by random drop and shuffle, e.g., the patch in the left-up corner is reordered in Green, Depth, Blue, where the Red channel is dropped; Last, the visualization of the mixed image is shown.

distinct geometric variations on the 3D mesh. Similarly, human emotional variations can lead to changes in blood pressure, skin surface temperature, and heart rate, which are captured by physiology machines and thermal cameras.

Thanks to recently developed multi-modal databases[40], [45], [44], progress has been made by exploiting additional information in multi-modal learning on human emotion tasks. For example, Li et al. [17], [18] combined the 2D and 3D features for facial expression recognition. In AU detection, Zhang et al. [43] present a fusion network with visual and depth modalities and Yang et al. [41] include one more modality, which is the thermal image. All the mentioned work is designed as late fusion or middle fusion, where each modality feature was extracted by a separate encoder, and fused into the latent space. One advantage of the late fusion method is the ability to handle cases where one or more modalities are missing. However, these two-stream structure based methods not only increase the parameter size of network but also ignore the low-level interaction between the modalities. In addition, the most common backbone (e.g. ResNet [12], ViT [8]) is pretrained by RGB image, which is not appropriate to be fed with the

depth or thermal modalities directly. On the other hand, early fusion, as the simplest example of fusion by concatenating individual modality features, hasn't been fully explored in recent multimodal learning studies but is usually used as a baseline method for comparison. In recent early fusion works [34], [47] utilizing visual and depth modalities, the two modalities are simply concatenated by channel, which is an under-explored fusion approach.

To address these above problems, we propose a multi-modal self-supervised model named Multi-modal Channel-mixing Network (MCM), which aims to build a robust pre-trained model that learns features from two modalities but is able to use a single modality for downstream AU detection. First, the 4-channel input from the early fusion of visual depth is remixed by a patches channel mixing module to produce a 3-channel output. Figure 1 shows the overview structure of the channel mixing module. Similar to heavy spatial redundancy in an image, e.g., a missing patch can be recovered from neighboring patches [11], we believe the redundancy also occurs across the channel in visual-depth data. Therefore, the channel mixing module is designed to randomly drop one of the 4 channels and shuffle the remains in each patch, so that the 3-channel output can not only match all the backbone pre-trained on ImageNet but also can be adapted to self-supervised learning tasks, e.g. image reconstruction. Second, the mixed image is fed into a ViT-based masked encoder, where the fused latent feature is extracted. Finally, the latent feature combined with mask tokens is passed through two parallel ViT-based decoders to reconstruct back visual image and depth image. This architecture is inspired by recently released work masked autoencoder (MAE) [11], where we expand from single modality to multimodalities, from spacial mask to channel mask and from object recognition to facial action unit detection.

Compared with related work, our contributions are as follows:

- 1) A multimodal channel mixing scheme (**MCM**) has been proposed for building a multi-modal self-supervised pre-training framework. Such a novel scheme not only helps to learn a robust representation but also facilitates the multi-modal fusion.
- 2) We have also proposed a unified framework for both visual and depth modalities. Such a new framework is more effective and efficient than the conventional multimodal fusion strategies. Additionally, our proposed framework is able to perform well when one of the multi-modalities is missing.
- 3) Extensive experiments have been conducted on two public datasets (BP4D, DISFA) to evaluate the effectiveness of the proposed method. The results show that our model is comparable or superior the state-of-the-art baseline methods.

II. RELATED WORK

A. AU Recognition

Automatic facial action recognition can be roughly categorized into single-modality-based methods and multi-modality-based approaches. The most commonly used modality is visual RGB image and a broad range of previous works [46], [19], [36], [33], [37], [20] has studied to use of a region of interest (ROI), image patches, facial landmarks, heat-map, attention mechanism, and other methods to localize detailed facial parts and learn discriminative feature representations. Considering the structural information and dependencies among different AUs on human faces, some recent works [15], [42], [21], [43] utilized the self-attention mechanism of transformer [39] to learn the semantic dependency among different AUs.

B. Multi-modal Learning

In the past decade, multi-modal learning has been studied on both facial expression recognition and action unit detection tasks. Li et al. [18] proposed a deep fusion network to learn the optimal combination weights of 2D and 3D facial representations for multi-modal 2D+3D FER. Researchers [14] proposed a method to utilize RGB-Thermal-Depth images for pain estimation. Li et al. [22] explained that EEG signals show a strong correlation with facial actions and eye blinking of both posed and spontaneous expressions. They utilize the early fusion of EEG feature and RGB feature to boost both posed and authentic facial actions detection. Liu et al. [24] designed a crossmodal translation network encoding the RGB images to reconstruct thermal images, which is an end-to-end model for AU detection. Yang et al. [41] proposed a model called AMF, which included a feature scoring module to select the most relevant feature representations from different modalities. The transformer-based [39] attention mechanism has been widely applied in multi-modal features fusion. For example, MulT [38] first attempted to fuse multi-modalities by transformer, which was applied to image, audio, and text. TransFuser [30] incorporates the global context of the 3D scene into the feature extraction layers of different modalities. Researchers [43] approach RGB-Depth features fusion by utilizing multi-head fusion attention to fuse AU features of two modalities in a transformer.

Recently, the line between multimodal representation and fusion has been blurred for models such as deep neural networks where representation learning interacts with classification or regression objectives [2]. Hence, we refer to early fusion as the immediate integration of the data source or feature from the extractor, often simply by concatenating them into a single vector as the input to the learning model. Compared to the number of late fusion works, only a few works utilize the early fusion strategy, e.g., [34], [47], [22]. One disadvantage of early fusion is the trained model usually can not handle the missing modality.

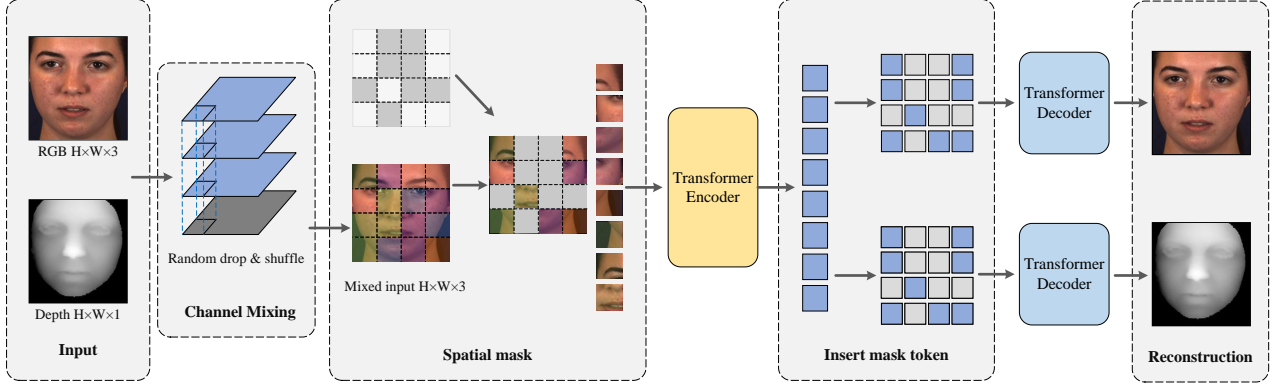


Fig. 2: An overview of the proposed Multi-modal Channel-mixing (MCM) Network, which is a multi-modal reconstruction network as a pre-train model for AU detection. In this model, two modalities are fused by channel and randomly remove from one channel. Then a large subset of random image patches is masked out. The encoder is applied to the remaining subset of visible patches. Two subsets of masked tokens combined with the shared visible encoder patches are proceeded by two small decoders to reconstruct two modalities respectively.

C. Masked Image Encoding

Inspired by the success of the masked language model [7], [31], [32], [4] in NLP, masked image encoding methods of self-supervised learning have been significantly improved in computer vision, often focusing on different pretext tasks for pre-training. BEiT [3] design an autoencoder network similar to BERT [7] with the ViT encoder and discrete image token. MAE [11] proposed another ViT backbone network that only encodes the visible patches and inserts masked tokens in decoding for reconstruction, which speeds up the training process. Inspired by MAE, we propose a multimodal channel mixing (MCM) module for the multi-modal self-supervised pre-training framework. **Differ** from the previous late fusion works, our method only includes one encoder for multimodality; **Differ** from the early fusion works, our downstream model can be fed with only one modality.

III. METHODOLOGY

In this section, we describe our method in detail, including Channel-Mixing Module, Masked Autoencoder, and AU detection network. The overall pipeline of our framework is illustrated in Figure 2. Encoder and decoders are based on ViT-Base and designed asymmetrical, i.e., 12, 8, and 4 layers in the encoder, RGB decoder, and Depth decoder respectively.

A. Channel-Mixing

We have visual image I_v and its corresponding depth image I_d , so the fused image is $I_f = I_v \oplus I_d$, where \oplus represents concat by channel. Then the fused image $i_f \in \mathbb{R}^{H \times W \times C}$ is split to patches $i_p \in \mathbb{R}^{L \times (p^2 \cdot C)}$, where (H, W) is its resolution, C is the number of channels ($C = 4$ in our task), (P, P) is the resolution of each image patch, and $L = HW/P^2$ is the resulting number of patches [8]. Then each patch is randomly dropped with one channel and then be shuffled in channel, so the channel-mixing image set is

$I_{mix} = \{i_{mix}\}$, where $i_{mix} \in \mathbb{R}^{L \times (p^2 \cdot (C-1))}$. Please see in Figure 1.

The proposed channel mixing module has the following advantages:

- 1) It downsamples the fused modality to 3 channels, which can take advantage of the large pre-trained backbone, allowing the AU detection model be fed with different modalities.
- 2) It increases the difficulty of the self-supervised learning task so that the network focus on both spatial and channel information.
- 3) The encoder is guided by the reconstruction task to learn the most relevant latent feature for both two modalities, resulting in an effective and robust representation.

B. Spatial Mask

We remove certain patches by random sampling based on a uniform distribution. By using uniform distribution, it has the potential to mask more patches near the center of the image, where the face is located. With high masking rates, redundancy is largely eliminated, resulting in a task that is not easily solved by visible neighboring patches inference. Since the following encoder proceeds with only unmasked patches, it speeds up the training process.

C. ViT Encoder

Our encoder is a ViT [8], and only proceeds with the visible, unmasked patches. As in a standard ViT, the patches are embedded by linear projection, and added with position embedding. Unlike using learnable 1D position embedding in the standard ViT, we use the 2-D sine-cosine variant [5] for position embedding. The embedding is then encoded by a stack of Transformer blocks following the design in [8]. Let w_l be the encoded features at the l -th layer in transformer blocks, W_0 being the input layer. The features at the l -th

layer are obtained by applying a transformer block defined as:

$$w'_l = F_{LN}^l(w_{l-1} + F_{MSA}^l(w_{l-1})) \quad (1)$$

$$w_l = F_{LN}^l(w'_l + F_{FF}^l(w'_l)) \quad (2)$$

where $F_{MSA}(\cdot)$ is the multi-head self-attention, F_{LN} is LayerNorm, and F_{FF} is a fully connected feed-forward network. We apply the ViT-base with 12 blocks and 512-dim as the encoder in our model. Different from previous multi-modal AU detection works [41], [43], there's only one encoder for two modalities in the proposed network.

D. ViT Decoder

Since we have two modalities of reconstruction task, two decoders are involved in our network. The inputs of two decoders $De = \{de_v, de_d\}$ are consisting of the shared encoded visible patches e , and two modalities mask tokens $\{m_v, m_d\}$, so that we have $de_v = \{e, m_v\}$, $de_d = \{e, m_d\}$. Each mask token is a shared embedding vector that represents a missing patch to be predicted in each decoder. Following the mask token design in [11], where removing the mask token from the encoder can not only improve the accuracy but also speed up the training process. The decoder position embeddings are also added to the input, otherwise, it would have no information about their location in the image. The decoder has another stacks of Transformer blocks, which are also defined as Equation.1 and Equation.2. The last layer of a decoder is a linear projection whose number of output channels equals the number of pixel values in a patch. The decoders are only used during pre-training to conduct the reconstruction tasks and only the encoder is used for downstream AU detection.

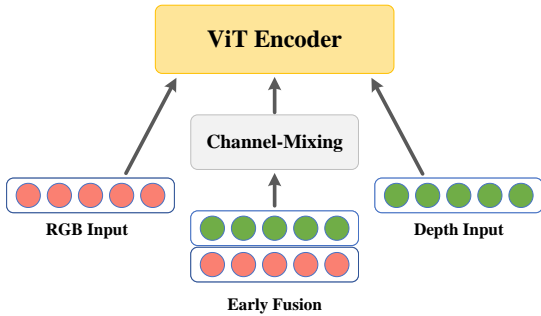


Fig. 3: Overview of how a single encoder accepts different modalities inputs on AU detection. Note that the inputs are exclusive, i.e., RGB or Depth, or Early Fusion.

E. AU Detection

Then we do supervised training to evaluate the representations from the encoder with end-to-end fine-tuning on AU detection. As we mentioned above, our model can accept mixed images as well as single modal images, where input $x \in \{I_v, I_d, I_{mix}\}$. Figure 3 shows how multi-modalities are fed into a single ViT encoder on AU detection. As a multi-label task, AU detection faces the common problem of

data unbalances. Hence, we apply the weighted binary cross-entropy (BCE) loss functions. The AU_k occurrence probability function $P(AU_k)$ and the correlate positive weight p_k of weighted BCE are given as:

$$P(AU_k) = \frac{\sum_{i=1}^N y_k^i}{\sum_{i=1}^N \sum_{k=1}^C y_k^i} \quad (3)$$

$$p_k = \frac{P(AU_k)}{\min\{P(AU_1), \dots, P(AU_C)\}} \quad (4)$$

where N is the total number of training set, C is the number of AUs. Then the weighted BCE loss is defined:

$$\mathcal{L} = -\frac{1}{N} \sum_{i=1}^N \sum_{k=1}^C (p_k \times y_k^i \times \log(\hat{y}_k^i) + (1 - y_k^i) \times \log(1 - \hat{y}_k^i)) \quad (5)$$

where y_k^i and \hat{y}_k^i represent the ground truth label and prediction for AU_k respectively.

IV. EXPERIMENT

Our self-supervised pre-trained model is training on the BP4D [44], where all the frames are extracted (with/without AU notation). We split all frames of the datasets into train and validate by 90% and 10%. The pre-training needs two modalities for input, that are, RGB and Depth. Then we employ supervised training by finetuning to evaluate the learned representations on AU detection.

Through our experiments, we aim to address the research questions with respect to following four aspects: **RQ1:** *Can our proposed method meet or outperform the state-of-the-art baseline methods?* **RQ2:** *Will fuse multiple modalities be more effective?* **RQ3:** *What is the impacts of different mask ratio for image reconstruction and down-stream task?* **RQ4:** *Why our model is more effective than the original MAE structure?*

A. Data

1) **BP4D** [44]: It contains 41 subjects (23 females and 18 males) captured in laboratory environments. There are 8 tasks designed to elicit different spontaneous emotions. In the total of all the 41×8 sequences, the number of all frames is around 360,000. Expert coders select the most expressive 20s of each video clip for AU coding, resulting in 140,000 labeled frames. We use 90% of all the frames in pre-training and only the labeled frames in fine-tuning AU detection. In the AU detection experiments, following the work [19], we split them into subject-exclusive 3-fold with 12 AUs for a fair comparison with state-of-the-art algorithms. Besides the visual images, the database provides the corresponding 3D face meshes as well.

2) **DISFA** [28]: It contains videos from the left view and right view of 27 subjects (12 females, 15 males). 12 AUs are labeled with AU intensity from 0 to 5, resulting in around 130,000 AU coded images. We choose 8 of 12 AUs from the left camera with AU intensities higher or equal to 2 as positive samples and the rest as negative samples. The

recognition model trained on BP4D is then fine-tuned to the DISFA dataset, which is following the setting in [19], [16]. F1-score is reported based on subject-exclusive 3-fold cross-validation.

B. Implementation details

1) *Pre-training*: Following the standard ViT architecture, we use ViT-base as the encoder and decoders, where 12 layers in the encoder, 8 and 4 layers in decoders for RGB and Depth respectively. The pre-trained weights from [11] on ImageNet are used for our encoder. Optimizer Adamw [26] with learning rate $2.e-4$, weight decay 0.05, and momentum (0.9, 0.95). We train 30 epochs with batch size 64 where the warmup epoch [10] is set with 5 and then perform cosine decay [25] with minimal lr by $1.e-6$.

2) *Fine-tuning*: The drop path [13] for ViT to 0.1 and layer-wise lr decay [3] is 0.75. Optimizer Adamw [26] with learning rate $4.e-4$, weight decay 0.05, and momentum (0.9, 0.99). We set the batch size to 64, train 5 epochs with 1 epoch warmup, and then use the cosine decay. In addition, the minimum lr was set to $1.e-6$, and when the 2nd epoch starts, the lr is reduced by a factor of 10.

C. Comparison with related methods

1) *RQ1 Single-modal results*: Our approach allows the use of a single modality in AU detection. Hence, we first compare our method to the state-of-the-art algorithms on RGB modality in terms of F1-score. Methods included on BP4D are EAC[19], DSIN[6], JAA-Net[33], SRERL[16], HMP-PS [35], SEV-Net[42], FAUT [15] MFT [43], and PIAP-DF [37]. The top section in Table I shows the results of visual images on BP4D, where our method achieves the best performance. Specifically, our method outperforms the SOTA methods in recognizing AU4, AU15, AU17, AU23, and AU24. To evaluate our method on Depth modality, we compare with [43] and Resnet-18, Resnet-50, as the baseline functions, where our method outperforms the state of the art. The result is reported in the bottom section of Table I.

Table II provides the results on the DISFA dataset. For DISFA, following the protocol in [19], [16], we do not train the model from scratch, but fine-tune the model trained on BP4D. Our method is comparable with the state-of-the-art method.

2) *RQ2 Multi-modal results*: Since our method also accepts fused channel-mixing feature as the input, we compare our method with the state-of-the-art multi-modal methods, i.e., MTUT [1], TEMT-Net [24], AMF [41], and MFT [43]. The F1-score of MTUT and TEMT-Net are reported in the work [41], where the author implemented them with the fusion of RGB and Depth. The results on BP4D are shown in Table III. Our method outperforms all the related methods and achieves the highest F1-score at 67.4%, which is 5.2% higher than MTUT, 4.2% higher than TEMT-Net, 2.6% higher than MFT, and 1.6% higher than AMF. In terms of 12 AUs, our method performs best in 6 AUs: AU1, AU7, AU14, AU17, AU23 and AU24. Furthermore, the fusion feature with channel-mixing also surpasses the performance

of all the methods on a single modality. Thus validating that using multiple modalities is more effective than a single modality.

D. Ablation Studies

1) *RQ3 Image reconstructions*: Figure 4 show reconstructions result on BP4D validation sets by different mask ratios, i.e., 50%, 75% and 90%. The reconstructions are generated by the pre-trained model with 50% masks. Our proposed method works well for the multi-modalities reconstruction task. The reconstruction qualities are decreased as the mask ratio is increased, especially in the mouth and eyes areas.

We also conducted experiments to evaluate the reconstruction results of our method across datasets, that is, generating visual images on DISFA. Since there's no depth modality in DISFA, we set the depth to zeros and then reconstruct from the pre-trained model on BP4D with mask 0.5. The result is shown in Figure 5. The reconstruction on DISFA is not as good as on BP4D, which could be caused by the following reasons. First, the image color in DISFA is biased, i.e., the distribution of the image ranges from warm to cool colors, which is much more deviated than BP4D. See the enormous difference in color between rows 1 and 2 in Figure 5. Second, the missing depth modality, where zeros are mixed with RGB, decreases the performance of reconstruction. However, the semantic information of the face, e.g., eyes, nose, and mouth, is well reconstructed, see in Figure 5.

2) *RQ3 Mask ratio and Training epoch in pretrain*: First, the ablation study of training epochs in pre-training is based on a 50% mask, where the results in multi-modalities are shown in Figure 6a in terms of average F1 scores. Performance steadily improved during the training process and reached its optimum after the 25th epoch. Our experiments thus far are based on the pre-training model on epoch-25.

Then we evaluate the masking ratio influence on downstream AU detection performance, see in Figure 6b. The optimal ratio is from 25% to 50%, when the ratio is greater than 50%, the f1 score is decreasing. Hence, we set the masking ratio by 0.5 and has reported the result of the experiments.

3) *RQ4 Effectiveness of Channel-Mixing on AU detection*: As an extension of the MAE, we carefully analyze the contribution of our proposed Channel-Mixing (CM) module by conducting comparison experiments on BP4D dataset. The proposed CM module is applied in both pre-training and finetuning stages on multi-modal learning. Table IV shows the performance of various comparisons in terms of the F1-score of 12 AUs. We first examine the CM module in the pre-train stage, where we use MAE as the baseline, see the Pretrain section in Table IV. Applying the proposed channel-mixing achieves a noticeable increase at 0.7%, 0.4%, and 1.1% in RGB, Depth, and Early Fusion (EF) respectively, leading to an improvement over the SOTA.

Then we use the pretrained ViT-Base model in MAE as the baseline to evaluate the CM module in fine-tune stage, and the results are shown in the Finetune section of Table IV. The early fusion is 4 channels as the input of

TABLE I: F1 scores of single modality on the BP4D. Bracketed and bold numbers indicate the best performance; bold numbers indicate the second best.

Methods	Modal	AU1	AU2	AU4	AU6	AU7	AU10	AU12	AU14	AU15	AU17	AU23	AU24	Avg
EAC	RGB	39.0	35.2	48.6	76.1	72.9	81.9	86.2	58.8	37.5	59.1	35.9	35.8	55.9
DSIN	RGB	51.7	40.4	56.0	76.1	73.5	79.9	85.4	62.7	37.3	62.9	38.8	41.6	58.9
JAA-Net	RGB	47.2	44.0	54.9	77.5	74.6	84.0	86.9	61.9	43.6	60.3	42.7	41.9	60.0
SRERL	RGB	46.9	45.3	55.6	77.1	78.4	83.5	87.6	63.9	52.2	63.9	47.1	53.3	62.9
HMP-PS	RGB	53.1	46.1	56.0	76.5	76.9	82.1	86.4	64.8	51.5	63.0	49.9	54.5	63.4
SEV-Net	RGB	[58.2]	[50.4]	58.3	[81.9]	73.9	[87.8]	87.5	61.6	52.6	62.2	44.6	47.6	63.9
FAUT	RGB	51.7	49.3	[61.0]	77.8	79.5	82.9	86.3	[67.6]	51.9	63.0	43.7	56.3	64.2
MFT	RGB	49.6	48.1	59.9	78.4	78.0	83.7	87.9	62.0	55.3	61.8	50.9	54.9	64.2
PIAP-DF	RGB	55.0	50.3	51.2	80.0	[79.7]	84.7	[90.1]	65.6	51.4	63.8	50.5	50.9	64.4
Ours (MCM)	RGB	55.9	49.8	[61.0]	79.9	77.5	84.2	89.0	63.6	[56.6]	[65.5]	[51.2]	[60.7]	[66.2]
ResNet-18	Depth	40.9	40.7	56.9	77.1	76.7	79.8	88.1	58.8	48.2	60.8	49.4	46.0	60.3
ResNet-50	Depth	[44.5]	[41.3]	[57.2]	76.5	72.6	80.9	86.8	54.3	50.2	62.7	48.1	44.5	60.0
MFT	Depth	38.6	37.3	44.2	[84.2]	[89.0]	[89.7]	[89.2]	[79.8]	44.7	46.0	[53.2]	37.0	61.1
Ours (MCM)	Depth	44.3	40.8	51.3	77.8	70.9	82.9	87.3	65.5	[50.8]	[63.1]	48.1	[54.5]	[61.4]

TABLE II: F1 scores of single modality on DISFA dataset. Bracketed and bold numbers indicate the best performance; bold numbers indicate the second best.

Methods	Modal	AU1	AU2	AU4	AU6	AU9	AU12	AU25	AU26	Avg
EAC	RGB	41.5	26.4	66.4	50.7	[80.5]	[89.3]	88.9	15.6	48.5
DSIN	RGB	42.4	39.0	68.4	28.6	46.8	70.8	90.4	42.2	53.6
JAA-Net	RGB	43.7	46.2	56.0	41.4	44.7	69.6	88.3	58.4	56.0
SRERL	RGB	45.7	47.8	59.6	47.1	45.6	73.5	84.3	43.6	55.9
SEV-Net	RGB	[55.3]	53.1	61.5	53.6	38.2	71.6	[95.7]	41.5	58.8
HMP-PS	RGB	38.0	45.9	65.2	50.9	50.8	76.0	93.3	[67.6]	61.0
FAUT	RGB	46.1	48.6	[72.8]	[56.7]	50.0	72.1	90.8	55.4	61.5
PIAP	RGB	50.2	51.8	71.9	50.6	54.5	79.7	94.1	57.2	[63.8]
Ours(MCM)	RGB	51.7	[59.8]	63.8	[56.7]	37.8	81.5	88.2	62.6	62.7

TABLE III: F1 scores of two fused modalities on the BP4D dataset. Bracketed and bold numbers indicate the best performance; bold numbers indicate the second best.

Methods	Modal	AU1	AU2	AU4	AU6	AU7	AU10	AU12	AU14	AU15	AU17	AU23	AU24	Avg
MTUT	Fusion	51.3	50.2	[62.2]	77.2	71.7	83.8	88.2	61.4	54.3	57.9	45.8	42.2	62.2
TEMT-Net	Fusion	53.7	47.1	60.5	77.6	75.6	84.8	87.4	67.0	57.2	61.3	44.7	41.6	63.2
AMF	Fusion	55.1	58.3	62.0	[82.5]	75.6	[87.2]	[89.6]	60.9	[59.1]	62.4	45.0	52.0	65.8
MFT	Fusion	51.6	49.2	57.6	78.8	77.5	84.4	87.9	65.0	56.5	64.3	49.8	55.1	64.8
Ours(MCM)	Fusion	[59.1]	51.0	61.8	80.4	[77.8]	84.5	88.8	[67.2]	56.5	[67.7]	[53.1]	[60.5]	[67.4]

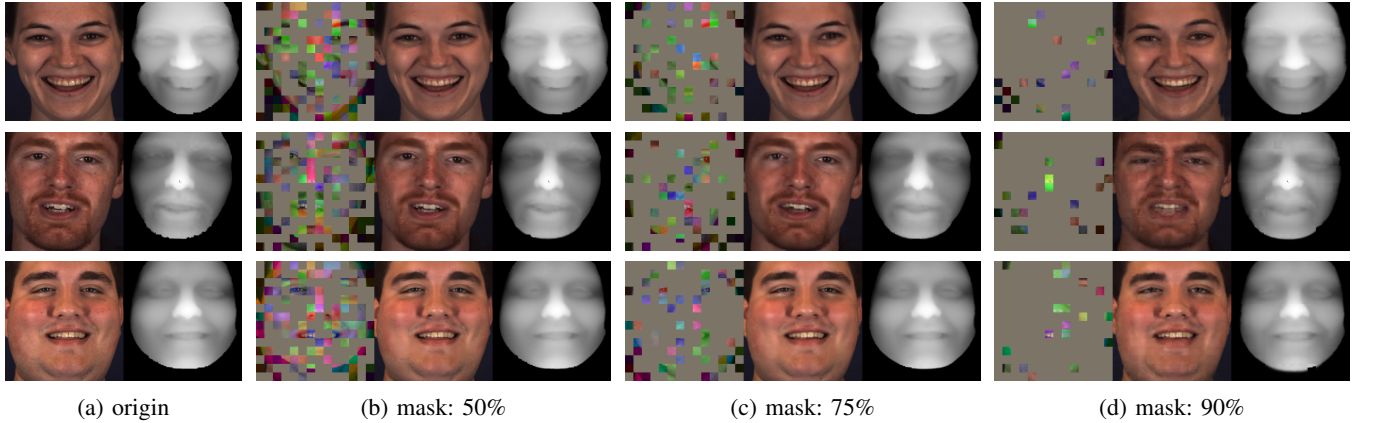


Fig. 4: Visualization of the reconstructed images on the BP4D dataset with different mask ratios. Four subjects are shown in 4 rows, where (a) shows origin RGB and Depth. The left picture in (b, c, and d) shows the masked channel-mixing image, the middle shows the reconstruction of RGB, and the right shows the reconstructions of Depth.

ViT, but the pretrained parameters from Imagenet are for 3 channels. To utilize the pretrained parameters, we apply a 1x1 convolutional layer to 3 channels before the embedding.

In original ViT, performance in RGB achieves the best, which is better than multimodal early fusion. However, the EF outperforms the RGB modality by directly utilizing the CM

TABLE IV: Ablation study of the effectiveness of proposed Channel-Mixing module on BP4D database. EF: Early Fusion; CM: Channel-Mixing. F1 scores in terms of 12 AUs are reported for different variants on the BP4D. A noticeable improvement is shown by using CM in two stages of Pretrain and Finetune.

Stage	Modal	CM	AU1	AU2	AU4	AU6	AU7	AU10	AU12	AU14	AU15	AU17	AU23	AU24	Avg
Pretrain	RGB	✗	55.5	50.3	60.2	79.3	75.9	82.6	88.5	62.7	53.7	65.2	52.2	59.5	65.5
	RGB	✓	55.9	49.8	61.0	79.9	77.5	84.2	89.0	63.6	56.6	65.5	51.2	60.7	66.2
	Depth	✗	44.5	41.4	51.0	77.5	69.8	82.1	87.2	62.1	48.3	65.7	48.7	53.1	61.0
	Depth	✓	44.3	40.8	51.3	77.8	70.9	82.9	87.3	65.5	50.8	63.1	48.1	54.5	61.4
	EF	✗	56.0	48.5	62.2	80.6	76.8	84.3	88.8	66.9	54.1	67.3	53.2	56.7	66.3
	EF	✓	59.1	51.0	61.8	80.4	77.8	84.5	88.8	67.2	56.5	67.7	53.1	60.5	67.4
Finetune	RGB	✗	43.9	42.9	51.1	78.9	77.1	83.2	87.6	69.6	51.9	60.7	46.2	58.8	62.7
	Depth	✗	40.6	36.7	50.8	78.8	72.1	81.8	87.8	68.1	50.0	61.7	47.0	55.3	60.9
	EF	✗	44.0	42.7	48.5	79.0	76.7	83.2	87.8	69.0	52.3	63.1	48.8	54.7	62.5
	EF	✓	47.9	45.8	48.9	78.9	77.6	84.2	88.0	68.4	52.0	61.6	46.8	55.9	63.0

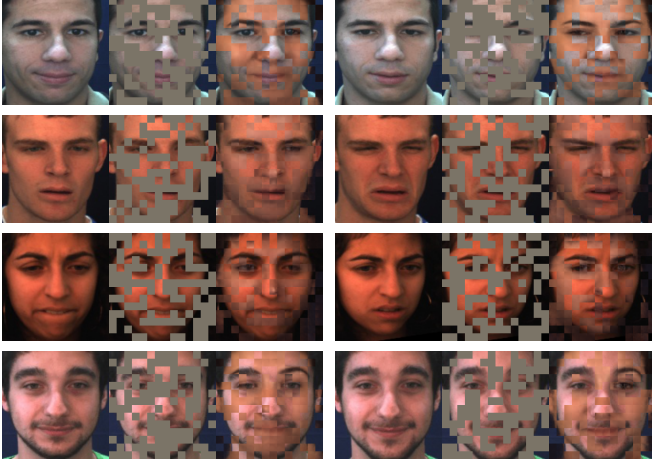


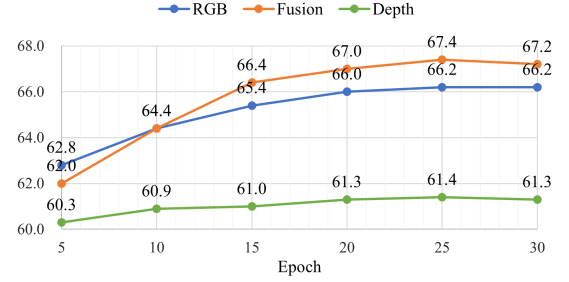
Fig. 5: Visualization of cross-dataset visual images reconstruction. The examples are reconstructed from the DISFA dataset using a pre-trained model on the BP4D dataset with a mask ratio of 0.5.

module.

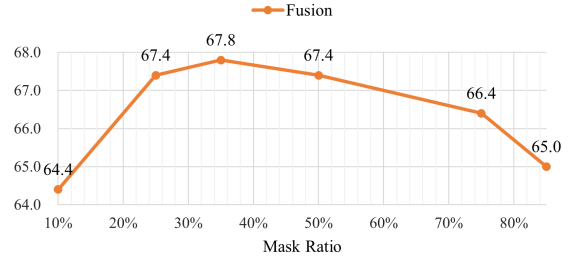
MAE in Pretrain improves more clearly because, in the pretrain task, channel mixing features are reconstructed through encoder and Decoder, where the channel information is well utilized to generate the lost channel. However, the mixing feature in ViT is fed directly to the network for AU pattern learning. In summary, Table IV shows the considerable improvement of using the proposed channel mixing module on the same architecture.

V. CONCLUSION

This paper has proposed a novel multi-modal self-supervised method, which utilizes visual and depth modalities for training a reconstruction network as a pre-trained model. We have explored the channel information fusion by designing a channel-mixing module, which empowers our method to be fed with either single modality or multimodalities by a single-stream encoder. Our proposed method is evaluated on AU detection on two widely used facial expression databases, BP4D and DISFA, and the performances meet and exceed the state-of-the-art results of the peers. Meanwhile, our results show the effectiveness of



(a) Finetune performance on various pretraining epochs, where a noticeable improvement along epochs.



(b) Finetune performance on various mask ratio of pretraining model.

Fig. 6: (a) F1 scores are reported by the model trained on BP4D with 50% mask. (b) F1 scores in fusion are reported by the model trained on BP4D with epoch-25.

multi-modal fusion, which performs noticeably better than single modality. The ablation experiments demonstrate the efficiency and robustness of the proposed channel mixing module.

REFERENCES

- [1] M. Abavisani, H. R. V. Joze, and V. M. Patel. Improving the performance of unimodal dynamic hand-gesture recognition with multimodal training. In *Proceedings of the IEEE/CVF Conference on Computer Vision and Pattern Recognition*, pages 1165–1174, 2019.
- [2] T. Baltrušaitis, C. Ahuja, and L.-P. Morency. Multimodal machine learning: A survey and taxonomy. *IEEE transactions on pattern analysis and machine intelligence*, 41:423–443, 2018.
- [3] H. Bao, L. Dong, S. Piao, and F. Wei. BEiT: BERT pre-training of image transformers. In *International Conference on Learning Representations*, 2022.
- [4] T. Brown, B. Mann, N. Ryder, M. Subbiah, J. D. Kaplan, P. Dhariwal, A. Neelakantan, P. Shyam, G. Sastry, A. Askell, et al. Language mod-

- els are few-shot learners. *Advances in neural information processing systems*, 33:1877–1901, 2020.
- [5] X. Chen, S. Xie, and K. He. An empirical study of training self-supervised vision transformers. *arXiv preprint arXiv:2104.02057*, 2021.
 - [6] C. Corneanu, M. Madadi, and S. Escalera. Deep structure inference network for facial action unit recognition. In *Proceedings of the European Conference on Computer Vision (ECCV)*, pages 309–324. Springer International Publishing, 2018.
 - [7] J. Devlin, M.-W. Chang, K. Lee, and K. Toutanova. Bert: Pre-training of deep bidirectional transformers for language understanding. In *NAACL-HLT (1)*, 2019.
 - [8] A. Dosovitskiy, L. Beyer, A. Kolesnikov, D. Weissenborn, X. Zhai, T. Unterthiner, M. Dehghani, M. Minderer, G. Heigold, S. Gelly, et al. An image is worth 16x16 words: Transformers for image recognition at scale. In *International Conference on Learning Representations*, 2020.
 - [9] P. Ekman and E. L. Rosenberg, editors. *What the face reveals: Basic and applied studies of spontaneous expression using the Facial Action Coding System (FACS)*. Oxford University Press, 1997.
 - [10] P. Goyal, P. Dollár, R. Girshick, P. Noordhuis, L. Wesolowski, A. Kyrola, A. Tulloch, Y. Jia, and K. He. Accurate, large minibatch sgd: Training imagenet in 1 hour, 2017.
 - [11] K. He, X. Chen, S. Xie, Y. Li, P. Dollár, and R. Girshick. Masked autoencoders are scalable vision learners, 2021.
 - [12] K. He, X. Zhang, S. Ren, and J. Sun. Deep residual learning for image recognition. In *Proceedings of the IEEE Conference on Computer Vision and Pattern Recognition (CVPR)*, June 2016.
 - [13] G. Huang, Y. Sun, Z. Liu, D. Sedra, and K. Q. Weinberger. Deep networks with stochastic depth. In B. Leibe, J. Matas, N. Sebe, and M. Welling, editors, *Computer Vision – ECCV 2016*, pages 646–661. Springer International Publishing, 2016.
 - [14] R. Irani, K. Nasrollahi, M. O. Simon, C. A. Corneanu, S. Escalera, C. Bahnsen, D. H. Lundtoft, T. B. Moeslund, T. L. Pedersen, M.-L. Klitgaard, et al. Spatiotemporal analysis of rgb-dt facial images for multimodal pain level recognition. In *Proceedings of the IEEE Conference on Computer Vision and Pattern Recognition Workshops*, pages 88–95, 2015.
 - [15] G. M. Jacob and B. Stenger. Facial action unit detection with transformers. In *2021 IEEE/CVF Conference on Computer Vision and Pattern Recognition (CVPR)*. IEEE, 2021.
 - [16] G. Li, X. Zhu, Y. Zeng, Q. Wang, and L. Lin. Semantic relationships guided representation learning for facial action unit recognition. In *Proceedings of the AAAI Conference on Artificial Intelligence*, volume 33, pages 8594–8601, 2019.
 - [17] H. Li, H. Ding, D. Huang, Y. Wang, X. Zhao, J.-M. Morvan, and L. Chen. An efficient multimodal 2d+ 3d feature-based approach to automatic facial expression recognition. *Computer Vision and Image Understanding*, 140:83–92, 2015.
 - [18] H. Li, J. Sun, Z. Xu, and L. Chen. Multimodal 2d+ 3d facial expression recognition with deep fusion convolutional neural network. *IEEE Transactions on Multimedia*, 19(12):2816–2831, 2017.
 - [19] W. Li, F. Abtahi, Z. Zhu, and L. Yin. EAC-net: A region-based deep enhancing and cropping approach for facial action unit detection. In *IEEE International Conference on Automatic Face & Gesture Recognition (FG)*, 2017.
 - [20] X. Li, Z. Li, H. Yang, G. Zhao, and L. Yin. Your “attention” deserves attention: A self-diversified multi-channel attention for facial action analysis. In *2021 16th IEEE International Conference on Automatic Face and Gesture Recognition (FG 2021)*, 2021.
 - [21] X. Li, X. Zhang, T. Wang, and L. Yin. Knowledge-spreader: Learning facial action unit dynamics with extremely limited labels, 2022.
 - [22] X. Li, X. Zhang, H. Yang, W. Duan, W. Dai, and L. Yin. An eeg-based multi-modal emotion database with both posed and authentic facial actions for emotion analysis. In *2020 15th IEEE International Conference on Automatic Face and Gesture Recognition (FG 2020)*, 2020.
 - [23] Y. Li, J. Zeng, S. Shan, and X. Chen. Self-supervised representation learning from videos for facial action unit detection. In *2019 IEEE/CVF Conference on Computer Vision and Pattern Recognition (CVPR)*. IEEE, jun 2019.
 - [24] P. Liu, Z. Zhang, H. Yang, and L. Yin. Multi-modality empowered network for facial action unit detection. In *2019 IEEE Winter Conference on Applications of Computer Vision (WACV)*, pages 2175–2184. IEEE, 2019.
 - [25] I. Loshchilov and F. Hutter. Sgdr: Stochastic gradient descent with warm restarts, 2016.
 - [26] I. Loshchilov and F. Hutter. Decoupled weight decay regularization. In *International Conference on Learning Representations*, 2019.
 - [27] L. Lu, L. Tavabi, and M. Soleymani. Self-supervised learning for facial action unit recognition through temporal consistency. In *BMVC*, 2020.
 - [28] S. M. Mavadati, M. H. Mahoor, K. Bartlett, P. Trinh, and J. F. Cohn. DISFA: A spontaneous facial action intensity database. *IEEE Transactions on Affective Computing*, 4(2):151–160, 2013.
 - [29] X. Niu, H. Han, S. Yang, Y. Huang, and S. Shan. Local relationship learning with person-specific shape regularization for facial action unit detection. In *Proceedings of the IEEE Conference on Computer Vision and Pattern Recognition (CVPR)*, 2019.
 - [30] A. Prakash, K. Chitta, and A. Geiger. Multi-modal fusion transformer for end-to-end autonomous driving. In *Proceedings of the IEEE/CVF Conference on Computer Vision and Pattern Recognition*, pages 7077–7087, 2021.
 - [31] A. Radford, K. Narasimhan, T. Salimans, and I. Sutskever. Improving language understanding by generative pre-training. 2018.
 - [32] A. Radford, J. Wu, R. Child, D. Luan, D. Amodei, I. Sutskever, et al. Language models are unsupervised multitask learners. *OpenAI blog*, 1(8):9, 2019.
 - [33] Z. Shao, Z. Liu, J. Cai, and L. Ma. Deep adaptive attention for joint facial action unit detection and face alignment. In *Proceedings of the European conference on computer vision (ECCV)*, pages 705–720, 2018.
 - [34] H. Song, Z. Liu, H. Du, G. Sun, O. Le Meur, and T. Ren. Depth-aware salient object detection and segmentation via multiscale discriminative saliency fusion and bootstrap learning. *IEEE Transactions on Image Processing*, 26(9):4204–4216, 2017.
 - [35] T. Song, Z. Cui, W. Zheng, and Q. Ji. Hybrid message passing with performance-driven structures for facial action unit detection. In *Proceedings of the IEEE/CVF Conference on Computer Vision and Pattern Recognition (CVPR)*, pages 6267–6276, June 2021.
 - [36] E. Sánchez-Lozano, G. Tzimiropoulos, and M. Valstar. Joint action unit localisation and intensity estimation through heatmap regression. In *BMVC*, 2018.
 - [37] Y. Tang, W. Zeng, D. Zhao, and H. Zhang. Piap-df: Pixel-interested and anti person-specific facial action unit detection net with discrete feedback learning. In *Proceedings of the IEEE/CVF International Conference on Computer Vision (ICCV)*, 2021.
 - [38] Y.-H. H. Tsai, S. Bai, P. P. Liang, J. Z. Kolter, L.-P. Morency, and R. Salakhutdinov. Multimodal transformer for unaligned multimodal language sequences. In *Proceedings of the conference. Association for Computational Linguistics. Meeting*, volume 2019, page 6558. NIH Public Access, 2019.
 - [39] A. Vaswani, N. Shazeer, N. Parmar, J. Uszkoreit, L. Jones, A. N. Gomez, Ł. Kaiser, and I. Polosukhin. Attention is all you need. In *Advances in neural information processing systems*, pages 5998–6008, 2017.
 - [40] S. Wang, Z. Liu, Z. Wang, G. Wu, P. Shen, S. He, and X. Wang. Analyses of a multimodal spontaneous facial expression database. *IEEE Transactions on Affective Computing*, 4(1):34–46, 2012.
 - [41] H. Yang, T. Wang, and L. Yin. Adaptive multimodal fusion for facial action units recognition. In *Proceedings of the 28th ACM International Conference on Multimedia*, pages 2982–2990, 2020.
 - [42] H. Yang, L. Yin, Y. Zhou, and J. Gu. Exploiting semantic embedding and visual feature for facial action unit detection. In *Proceedings of the IEEE/CVF Conference on Computer Vision and Pattern Recognition*, pages 10482–10491, 2021.
 - [43] X. Zhang and L. Yin. Multi-modal learning for AU detection based on multi-head fused transformers. In *2021 16th IEEE International Conference on Automatic Face and Gesture Recognition (FG 2021)*. IEEE, 2021.
 - [44] X. Zhang, L. Yin, J. F. Cohn, S. Canavan, M. Reale, A. Horowitz, P. Liu, and J. M. Girard. Bp4d-spontaneous: a high-resolution spontaneous 3d dynamic facial expression database. *Image and Vision Computing*, 32(10):692–706, 2014.
 - [45] Z. Zhang, J. M. Girard, Y. Wu, X. Zhang, L. Yin, et al. Multimodal spontaneous emotion corpus for human behavior analysis. In *Proceedings of the IEEE conference on computer vision and pattern recognition*, pages 3438–3446, 2016.
 - [46] K. Zhao, W.-S. Chu, F. De la Torre, J. F. Cohn, and H. Zhang. Joint patch and multi-label learning for facial action unit detection. In *Proceedings of the IEEE Conference on Computer Vision and Pattern Recognition (CVPR)*, 2015.
 - [47] X. Zhao, L. Zhang, Y. Pang, H. Lu, and L. Zhang. A single stream network for robust and real-time RGB-d salient object detection. In *ECCV*. 2020.